Evaluation of Factors in the Preparation of Nano-Particles in a Super-Critical Anti-Solvent Process using 3D CFD Approach

Xiao Kefeng[1,2,3], Wang Weiqiang[1,3,*], Hu Dedong[3,4], Qu Yanpeng[1,3]

1. School of Mechanical Engineering, Shandong University, Jinan, China, 250061.
2. College of Chemistry and Pharmaceutical Science, Qingdao Agricultural University Qingdao, China, 266109.
3. Shanda-Lunan Research Institute of Supercritical Fluid Technology, Shandong University, Jinan, China, 250061.
4. The College of Electromechanical Engineering, Qingdao University of Science and Technology Qingdao, China, 266061.
* Correspondence author

***Abstract* – In this paper we use empirical formulae to compute Mean Particle Size (MPS) sprayed from a mixed nozzle, and the computational model of MPS in Supercritical Anti-Solvent (SAS) process is formulated. The model parameter values were obtained by Computational Fluid Dynamics (CFD) simulation of SAS process using Fluent software. The calculated data were used to analyse orthogonal results and compare them with experimental results. The calculated values of MPS in every treatment were very close to the experimental values. We conclude the calculated analysis results in the order of each factor of importance in preparation of Cefquinome by SAS process are: i) concentration of solution, ii) feeding speed of solution, iii) pressure and iv) temperature. The optimal conditions were: i) solution concentration was 100mg/ml, ii) solution flow speed was 1.5mL/min, iii) operating pressure was 13Mpa, and iv) operating temperature was 33℃. These results agreed with experimental results. Moreover, the calculated data was used to conduct univariate analysis and compare them with experimental data. The results showed that the trend obtained in this study of the impact of solution concentration, solution feeding speed and pressure on MPS were consistent with experimental analysis results. The trend of impact of temperature on MPS was slightly different with experimental analysis results. Modelling helps to study the process of preparation nano-drug in SAS process, optimize the process and scale-up it.**

Keywords - computational fluid dynamics; nanoparticle; cefquinome; supercritical antisolvent

I. INTRODUCTION

Most drug candidates are weak in aqueous solubility, which influenced greatly the biological activity and clinical application of drugs. According to Ostwald–reundlich equation, when the drug particle size is less than 1000 nanometer, The specific surface area of the drug would increase greatly and then the solubility would increase accordingly[1]. Reducing drug particle size became an effective method for solubility improvement [2, 3]. Several methods, including medium milling[4], high-gravity anti-solvent precipitation[5], micronization by supercritical fluid technology[6, 7] and so on, can be used to prepare nano-drug. In recent years, micronization by supercritical fluid technology has been studied widely in pharmaceutical industries [8-10]. Under decompression, supercritical fluids can be separated from both organic solvents and particles, which is one of the important advantages of the method. The other important advantage of the method is that the particle size and particle size distribution can be controlled by adjusting the pressure and/or temperature. In this process, supercritical fluid can act as solvent or antisolvent. According to the role difference of supercritical fluid, micronization by supercritical fluid technology can be classified into two types. The one is rapid expansion of supercritical solution(RESS), and the other is supercritical anti-solvent (SAS). For those drugs insoluble in supercritical fluid, SAS process has become the main technology to prepare nanoparticles, and this method was used in this study。

In SAS process, at close to the critical point of the mixture, the particles formed exhibit high sensitivity to changes of process parameters, such as solution flow rate, temperature or pressure. These parameters have a strong influence on the precipitated particle size. In literatures about preparation nanoparticles by using SAS process, contradictory results regarding the relation between the particle size and these process parameters can be found. Taking pressure as an example, Franceschi E et al.[11] thought that the increase of the operating pressure can lead to an increase in the particle size; Miguel F et al. showed different result that with the increase of pressure, the particle size decreased[12]; moreover, the study of Chang, Shan-Chun et al.[13] indicated that the change of pressure have no influence on the precipitated particle size. This is mainly because that the impact of these parameters on particle size are interrelated. The internal mechanism of the SAS process is very complex because it

involves the coupling of mass transfer, thermodynamics, and precipitation kinetics, which make it difficult to elucidate the underlying mechanisms that control particle size during SAS process. Experiment study can not entirely reveal these mechanisms. In previous work [14], we have studied the impact of four factors in SAS process for preparing Cefquinome Nanoparticles on particle size by orthogonal experiments. In order to further investigate the process, Computational fluid dynamics(CFD) was used to simulated the process on the basis of previous study. Mean particle size (MPS) was an important indicator in experiment analysis. The intention of this study was to establish a computation model for predicting MPS of prepared Cefquinome particles in SAS process combined with the experimental results, the simulation data and empirical formula of computing MPS for associated nozzle, and to verify the model by experimental results.

II. GOVERNING EQUATIONS AND METHODOLOGY

A. Governing Equation

In this CFD analysis, both SCF phase and solution phase are treated in an Eulerian framework. The primary phase is supercritical CO_2, and the dispersed phase is Cefquinome/DMSO solution.

The continuity equation is defined as Eq. (1).

$$\frac{\partial(\rho u)}{\partial x}+\frac{\partial(\rho v)}{\partial y}+\frac{\partial(\rho w)}{\partial z}=0 \quad (1)$$

where u, v, w are the component of velocity vector $\vec{u}$ in x, y and z direction respectively. ρ is the density of the mixture.

The momentum conservation equations are defined as Eq. (2) - Eq. (4).

$$\frac{\partial(\rho u)}{\partial t}+\mathrm{div}\left(\rho u\vec{u}\right)=\mathrm{div}(\mu\ \mathrm{grad}\,u)-\frac{\partial p}{\partial x}+s_u \quad (2)$$

$$\frac{\partial(\rho v)}{\partial t}+\mathrm{div}\left(\rho v\vec{u}\right)=\mathrm{div}(\mu\ \mathrm{grad}\,v)-\frac{\partial p}{\partial y}+s_v \quad (3)$$

$$\frac{\partial(\rho w)}{\partial t}+\mathrm{div}\left(\rho w\vec{u}\right)=\mathrm{div}(\mu\ \mathrm{grad}\,w)-\frac{\partial p}{\partial w}+s_w \quad (4)$$

where s_u, s_v and s_w are the generalized source term of the momentum conservation equations. s_u, s_v and s_w can be calculated by Eq.(5)- Eq.(7).

$$s_u=F_x+\frac{\partial}{\partial x}\left(\mu\frac{\partial u}{\partial x}\right)+\frac{\partial}{\partial y}\left(\mu\frac{\partial v}{\partial x}\right)+\frac{\partial}{\partial z}\left(\mu\frac{\partial w}{\partial x}\right)+\frac{\partial}{\partial x}(\lambda div\vec{u}) \quad (5)$$

$$s_v=F_y+\frac{\partial}{\partial x}\left(\mu\frac{\partial u}{\partial y}\right)+\frac{\partial}{\partial y}\left(\mu\frac{\partial v}{\partial y}\right)+\frac{\partial}{\partial z}\left(\mu\frac{\partial w}{\partial y}\right)+\frac{\partial}{\partial y}(\lambda div\vec{u}) \quad (6)$$

$$s_w=F_z+\frac{\partial}{\partial x}\left(\mu\frac{\partial u}{\partial z}\right)+\frac{\partial}{\partial y}\left(\mu\frac{\partial v}{\partial z}\right)+\frac{\partial}{\partial z}\left(\mu\frac{\partial w}{\partial z}\right)+\frac{\partial}{\partial z}(\lambda div\vec{u}) \quad (7)$$

Standard $k-\varepsilon$ model was used to simulate the turbulence of the flow. The governing equation groups are Eq. (8) and Eq. (9).

$$\frac{\partial(\rho k)}{\partial t}+\frac{\partial(\rho k u_i)}{\partial x_i}=\frac{\partial}{\partial x_i}\left[(\mu+\mu_t)\frac{\partial k}{\partial x_i}\right]+G_k-\rho\varepsilon \quad (8)$$

$$\frac{\partial(\rho\varepsilon)}{\partial t}+\frac{\partial(\rho\varepsilon u_i)}{\partial x_i}=\frac{\partial}{\partial x_i}\left[\left(\mu+\frac{\mu_t}{1.3}\right)\frac{\partial\varepsilon}{\partial x_i}\right]+\frac{1.44\varepsilon}{k}G_k-1.92\rho\frac{\varepsilon^2}{k} \quad (9)$$

Turbulent kinetic energy *k* can be obtained by Eq. (10).

$$k = \frac{3}{2}\left(\bar{u}_{ref} I\right)^2 \quad (10)$$

where $\bar{u}_{ref}$ is the average velocity of inlet. *I* is the turbulent intensity of inlet, which can be calculated by Eq. (11).

$$I = 0.16(\mathrm{R}_{eDH})^{-1/8} \quad (11)$$

Turbulent dissipation rate ε was calculated by Eq. (12) and Eq. (13).

$$l = 0.07L \quad (12)$$

$$\varepsilon = 0.09^{3/4}\frac{k^{3/2}}{l} \quad (13)$$

where, *L* is characteristic length, and is the diameter of inlet in this study.

B. Modelling of MPS

On the basis of the hypothesis of one droplet–one particle[14], MPS can be calculated by Eq.(14).

$$\frac{\pi}{6}D_c^3 = \frac{\pi}{6}D_s^3 \times \frac{C_c}{\rho_c} \quad (14)$$

After being simplified, Eq.(14)turned into Eq.(15), which was the final equation to calculate MPS.

$$D_c = D_s\sqrt[3]{\frac{C_c}{\rho_c}} \quad (15)$$

where, D_c is mean diameter of precipitated particles mm; D_s is mean diameter of solution droplets mm; C_c is the concentration of the solution mg/ml; ρ_c is the density of the solute, mg/ml;

The mean diameter of solution droplets D_s can be calculated by empirical formula. Because the nozzle used in this study is two-fluids out-mixed nozzle and The SAS process is also a spray process, the equation of calculating MPS of droplets in traditional out-mixed spray process [15] can act as basis equation in calculating MPS in SAS process. The basic equation is as Eq. (16).

$$D_s = 2600\left[\left(\frac{M_L}{M_a}\right)\left(\frac{\mu_a}{\rho_a v_a d_1}\right)\right]^{0.4} \quad (16)$$

where, M_L is the mass flow rate of solution kg/h; M_a is the mass flow rate of supercritical fluid kg/h; μ_a is the viscosity of supercritical fluid, Pa.s; ρ_a is the density of supercritical fluid, g/ml; v_a is the velocity of supercritical fluid, cm/s; d_1 is the diameter of the solution inlet cm;

In the hypothesis of one droplet–one particle, a part of agglomeration has been included in calculating MPS. Whereas, the pre-experimental results showed that calculated MPS was smaller than experimental MPS, which indicated that the agglomeration was greater than that included in the hypothesis. Therefore, a coefficient was needed to correct the effect of agglomeration on MPS. As mentioned in literature[17], the extent of particle agglomeration can be represented by agglomeration coefficient AF(50), given by:

AF(50) = diameter of medium-size aggregates/ mean equivalent diameter of particles (17)

where, diameter of medium-size aggregates is the diameter of 50% cumulative mass in particle size analysis. It can be concluded from Eq.(17) that the bigger AF(50) is, the more serious the agglomeration is. Generally, the AF(50) of superfine particles without special treatment in water is about 30[17]. In the model of this study, if the AF(50) was used directly in calculation, it will lead to repeat amendment about agglomeration. Therefore, a agglomeration correction coefficient *k* was employed to improve the accuracy of the model. Then, the Eq.(15) turned into Eq.(18). The meaning of *k* is that the hypothesis of the model was changed. That is, After being sprayed, the number of agglomerated droplets is *k*. The value of k can be obtained from pre-experiments and verified by experiments. In this study, the value of k was 16, determined by pre-experiments.

$$D_c = D_s\sqrt[3]{\frac{kC_c}{\rho_c}} \quad (18)$$

The equation of calculating MPS can be obtained from Eq.(16) and Eq.(18), shown as Eq.(19).

$$D_c = 2600\sqrt[3]{\frac{kC_c}{\rho_c}}\left[\left(\frac{M_L}{M_a}\right)\left(\frac{\mu_a}{\rho_a v_a d_1}\right)\right]^{0.4} \quad (19)$$

where, both agglomeration correction coefficient *k* and the density of the solute ρ_c are constants and is 16 and 2166.53 respectively. The concentration of the solution C_c , the mass flow rate of solution M_L and the diameter of the solution inlet d_1 can be obtained from operating conditions; the mass flow rate of supercritical fluid M_a was calculated by Fluent software and was obtained by Flux reports. The velocity of supercritical fluid v_a was also obtained from Fluent simulation. the density of supercritical fluid ρ_a was calculated by Peng-Robinson equation of state , shown as Eq.(20).

$$P = \frac{RT}{(V-b)} - \frac{a}{\left[V(V+b)+b(V-b)\right]} \quad (20)$$

Where

$$b = 0.07780\frac{RT_c}{P_c} \tag{21}$$

$$a = 0.45724\frac{(RT_c)^2}{P_c}\left[1 + m\left(1 - \sqrt{T_r}\right)\right]^2 \tag{22}$$

$$T_r = \frac{T}{T_c} \tag{23}$$

And

$$m = 0.37464 + 1.5422\omega - 0.26992\omega^2 \tag{24}$$

The critical pressure and temperature and acentric factor of CO_2 are: P_c=7.375MPa, T_c=304.2K and ω=0.225.

C. Model Analysis

The work of Xiao Kefeng et al. [14] was utilized as a reference to validate the model proposed herein. Nozzle and precipitator were the key parts of the experimental SAS device used in literature [14].

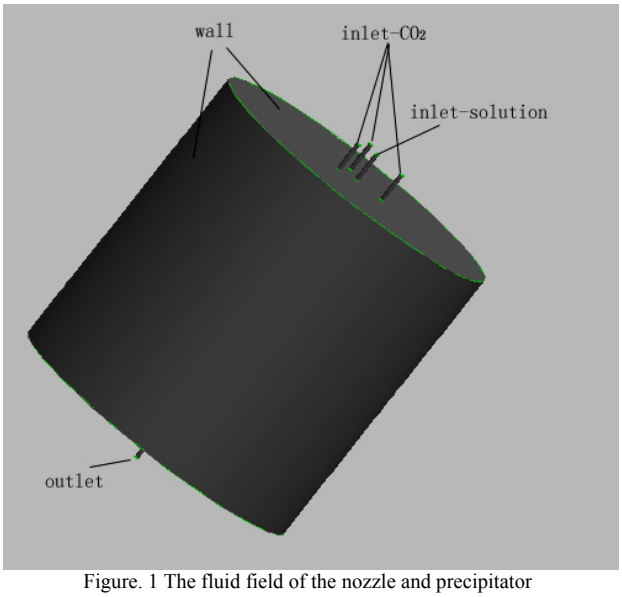

Figure. 1 The fluid field of the nozzle and precipitator

The fluid field detail of the nozzle and precipitator was shown in Figure 1 and the top view of the nozzle and precipitator can be seen in Figure 2. The nozzle concludes one inlet to feed solution and three inlets to feed supercritical fluid. The later three inlets were distributed evenly around the former inlet. At the bottom of the precipitator, there was an outlet. The supercritical fluid used in this study was supercritical CO_2 acting as antisolvent and Dimethyl sulfoxide (DMSO) acted as organic solvent. The experimental conditions investigated were same as that in literature [14].

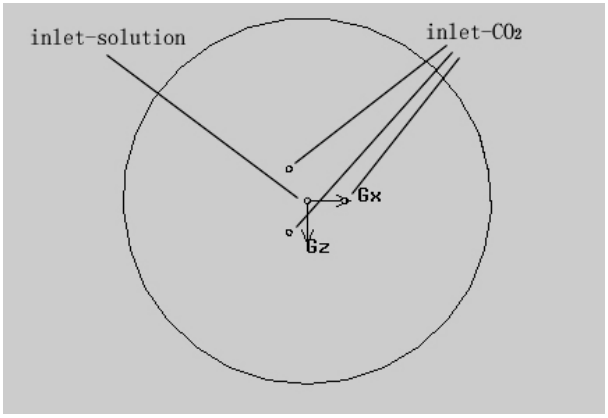

Figure. 2 Top view of the nozzle and precipitator

Tetrahedron elements and hexahedral wedge elements were included in the computational mixed mesh. The diameter of outlet was 1mm. 425894 mixed cells were included in the grid. In order to solve above Eqs.(1)-(14), ANSYS FLUENT 14.0, a commercial CFD software, was used. Fluent is a generic solver based on unstructured grids. In the software, two kinds of numerical methods can be selected: pressure-based solver and density-based solver. Pressure-based solver is suitable for incompressible flow and moderate compressible flow. This algorithm, a mature algorithm, conduct pressure correction on momentum equation, but not solved Navier-Stokes equations simultaneously. Density-based solver solves transient N-S equation directly and turn transient problem into the transient behavior of a time-marching. The steady-state solution converged is obtained with initial time marching. This algorithm is suitable for solving compressible flow in subsonic or supersonic. According to observation in experiment process and calculation, the flow in this study was not subsonic or supersonic. Therefore, pressure-based solver was selected and SIMPLEC algorithm was employed. After being read, the mesh was reordered several times until the bandwidth reduction was very low in order to optimize the grid.

Boundary conditions were shown in figure 1. The diameters of both CO_2 inlets and DMSO inlet were 0.3mm. For the CO_2 inlets, a simple pressure-inlet was selected and allowed to specify Gauge Total Pressure, Turbulent Kinetic Energy k and Turbulent Dissipation Rate ε. The volume fraction of DMSO was zero. For the solution inlet, velocity-inlet was selected and allowed to specify velocity magnitude of solution, turbulence intensity, hydraulic diameter and volume fraction of solution. For the outlet, pressure-outlet was employed. The gauge pressure of outlet was set to be 7.5Mpa. The factors and levels of the orthogonal array design used in literature [14] were shown in Table 1.

TABLE 1 FACTORS AND LEVELS OF THE ORTHOGONAL ARRAY DESIGN

Factor	Concentration Of Solution (Mg/Ml)	Solution Feeding Speed (Ml/Min)	Pressure (Mpa)	Temperature (℃)
1	100	0.5	10	33
2	200	1	13	38
3	300	1.5	16	43

III. RESULTS AND DISCUSSION

A. Analysis of Orthogonal Experiment by Calculated Data

The orthogonal experiment design and the level values used in literature [14] acted as basic conditions in the simulation of this study. The data of the flow in SAS process was obtained by CFD simulation. And then the MPS of every treatment was calculated by Eq.(19). The calculated MPS was compared with experimental data, as shown in Figure 3. It indicated that the calculated MPSs were all near the experimental values. Among these results, the gap between the calculated and experimental data in six treatments were within 9% and the change trend was similar. Which indicated that the accuracy of calculation was acceptable.

If calculated data can be used to analyze orthogonal experiment, it is of great significance for improve successful rate of experiments and decrease the cost of experiment. The calculated results of all treatments were used to analyze the SAS process by range analysis, and the analysis results was shown in Table 2.

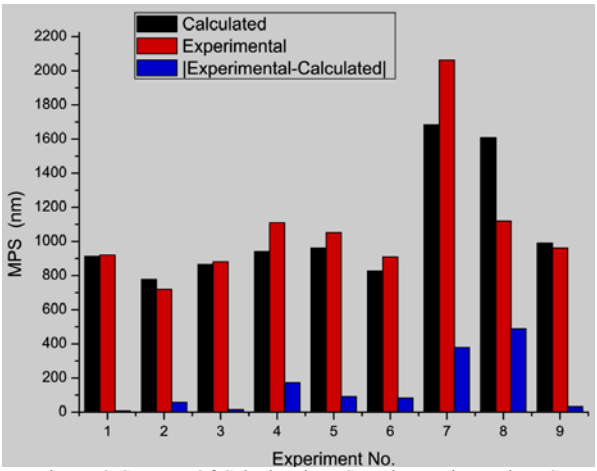

Figure. 3 Contrast Of Calculated MPS And Experimental MPS

It indicated that the range of the four factors were sorted in descending order as follow: A>B>C>D. Therefore, the order of these factors for importance in preparation Cefquinome by SAS process was as follow: concentration of solution, feeding speed of solution, pressure and temperature. It can also be determined from Table 2 that the optimal operating condition was $A_1B_3C_2D_1$. All the results were the same with experiment results in literature [14]. Through above mentioned analysis, it can be concluded that the trends of analysis results for both calculated data and experimental data were consistent and the data calculated by the model can be used in experiment pre-analysis.

TABLE 2 ANALYSIS OF L9(34) SIMULATION TEST RESULTS

run	A. Concentration of Solution (mg/ml)	B. Solution Feeding Speed (ml/min)	C. Pressure (Mpa)	D. Temperature (℃)	MPS (μm)
1	1	1	1	1	0.912
2	1	2	2	2	0.776
3	1	3	3	3	0.864
4	2	1	2	3	0.940
5	2	2	3	1	0.959
6	2	3	1	2	0.827
7	3	1	3	2	1.683
8	3	2	1	3	1.608
9	3	3	2	1	0.990
K1[a]	0.851	1.178	1.116	0.954	
K2	0.909	1.114	0.902	1.095	
K3	1.427	0.894	1.169	1.137	
R[b]	0.576	0.285	0.267	0.142	
Optimal Level	A1	B3	C2	D1	

[a] $K_i^A = \Sigma$(mean particle size at A_i) /3, the mean values of mean particle size for a certain factor at each level with standard deviation.
[b] $R_i^A = \max\{K_i^A\} - \min\{K_i^A\}$

B. *Univariate Analysis of Orthogonal Experiment by Calculated Data*

The trend of the effect of a factor on indicator can be obtained by analyze the average result value of the factor in different levels. In literature [14], the trends were analyzed by experimental data, which helped to instructing the further study of SAS process. In this study, the data calculated by new model was used to analyze the effect trends of the four factors on MPS. The effect trends obtained by calculated data was compared with experimental results, as shown in Figure 4-Figure 7.

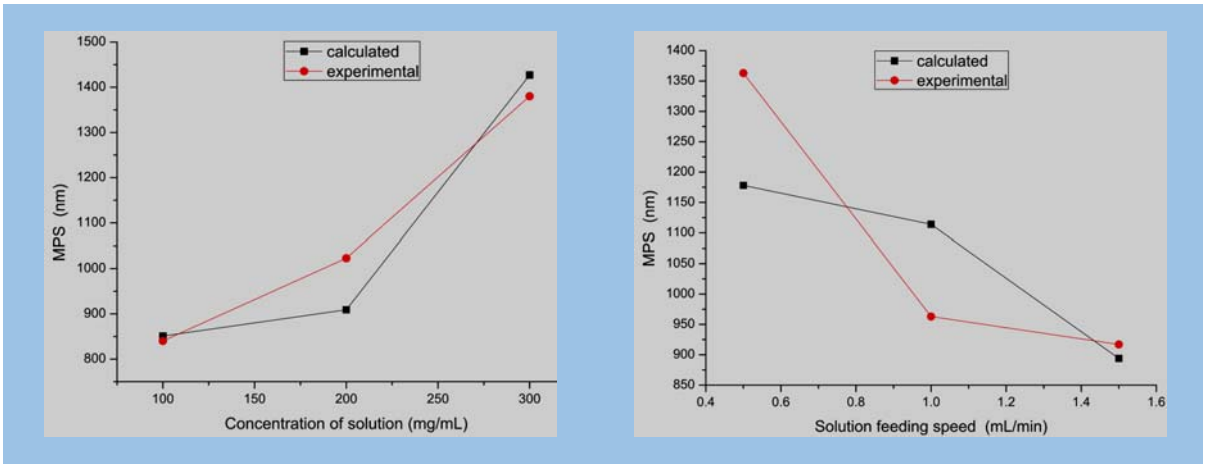

Figure. 4 Effect of solution concentration on MPS

Figure. 5 Effect of solution feeding speed on MPS

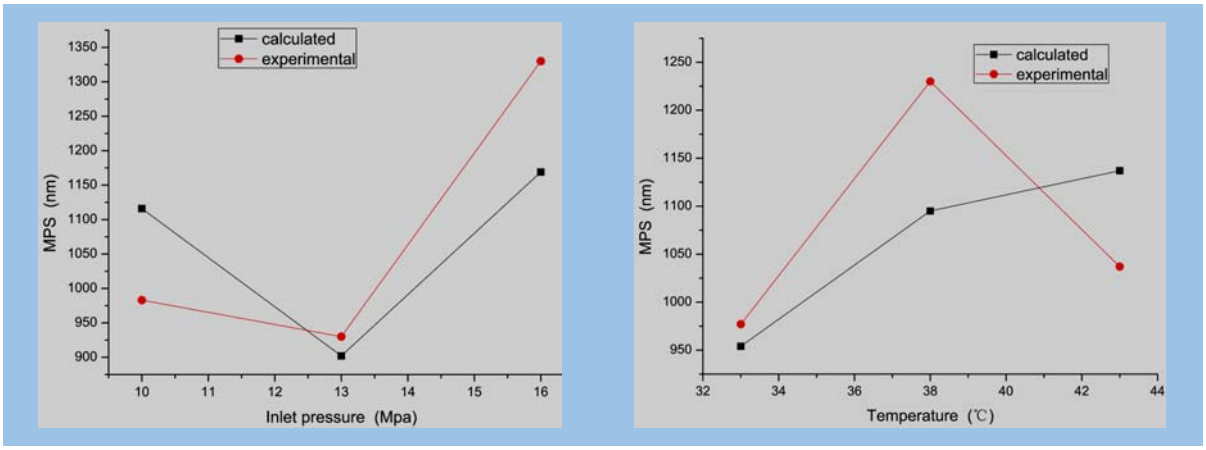

Figure. 6 Effect of inlet pressure on MPS

Figure. 7 Effect of temperature on MPS

It can be seen from Figure 4 that the MPS increased with the increase of solution concentration. The trends of calculated results were very similar with experimental results. Moreover, the calculated values in the three points were very close to experimental values. Therefore, it can be concluded that calculated data can be used to estimate the effect of solution concentration on MPS. It can be seen from Figure 5 that MPS decreased with the increase of solution feeding speed both for calculated values and experimental values. The trends were consistent, although gap still existed in some points. It can be seen from Figure 6 that the effect of pressure on MPS was complex. A lowest point appeared in the experiment interval. The reason is that the effect of precipitation pressure on the average diameter had a dual character [14]. It indicated that the changing tendency of the effect of pressure on MPS, obtained by calculated data, was consistent with that obtained by experimental data. From Figure 7, it was shown that the MPS increased with the increase of temperature by calculated data. Whereas, MPS appeared maximum value when the temperature was 38℃. There was a little difference between calculated data and experimental data. That might because that there was a little bug in the hypothesis of the model about temperature, or there was error about temperature in experiments. The problem would be solved in further study.

IV. CONCLUSIONS

On the basis of the empirical formula of computing mean particle size(MPS) for spraying by out-mixed nozzle, the computational model of MPS in supercritical anti-solvent (SAS) process was established. The values of parameters in the model were obtained by Computational fluid dynamics (CFD) simulation of SAS process using Fluent software. The calculated data were used to analyze orthogonal experiment and compare with experimental results. The calculated values of MPS in every treatment were very close to the experimental values in literature [14]. It can be concluded by calculated analysis results that the order of each factor for importance in preparation Cefquinome by SAS process is as follow: concentration of solution, feeding speed of solution, pressure and temperature. And the optimal conditions were that solution concentration was 100mg/ml, solution flow speed was 1.5mL/min, operating pressure was 13Mpa, and operating temperature was 33℃. These results were all the same with experimental results. Moreover, the calculated data was used to conduct univariate analysis and compared with experimental data. The results showed that the trend obtained in this study of the impact of solution concentration, solution feeding speed and pressure on MPS were consistent with experimental analysis results. Only the trend of impact of temperature on MPS was slightly different with experimental analysis results. It might because that the calculation model still need to be improved about temperature or there were error for temperature measurement in experiment. This problem would be solved in the future study. Although presented models were based on several simplifying assumptions and employed empirical equations. They can predict all basic trends observed in experiments although agreement of model predictions with experimental data is not always fully consistent. Modeling helps to study the process of preparation nano-drug in SAS process, optimize the process and scale-up it.

CONFLICT OF INTERESTS

The authors declare that there is no conflict of interests regarding the publication of this paper.

ACKNOWLEDGEMENTS

This work was financially supported by Science and Technology Development Plan of Shandong Province: Supercritical Fluid Dyeing Technology Research and Device Development (2014GGX108001).

REFERENCES

[1] Zhao X, Chen X, Zu Y, lynnetwwwdagriorglynnet. Recrystallization and Micronization of Taxol Using the Supercritical Antisolvent (SAS) Process[J]. *Ind Eng Chem Res*, 2012, 51(28): 9591-9597.

[2] Anand U, Ambarish J. Fabrication of starch-based microparticles by an emulsification crosslinking method[J]. *J Chem Pharm Res*, 2011, 3(6): 839-845.

[3] Domadia B A, Vaghela N R. Supercritical fluid extraction of lycopene from tomatos by using CO2 as a solvent: A review[J]. *J Chem Pharm Res*, 2013, 5(4): 188-191.

[4] Ain-Ai A, Gupta P K. Effect of arginine hydrochloride and hydroxypropyl cellulose as stabilizers on the physical stability of high drug loading nanosuspensions of a poorly soluble compound[J]. *Int J Pharm*, 2008, 351(1-2): 282-288.

[5] Chen J F, Zhang J Y, Shen Z G, lynnetwwwdagriorglynnet. Preparation and characterization of amorphous cefuroxime axetil drug nanoparticles with novel technology: High-gravity antisolvent precipitation[J]. *Ind Eng Chem Res*, 2006, 45(25): 8723-8727.

[6] Chen A Z, Li L, Wang S B, lynnetwwwdagriorglynnet. Nanonization of methotrexate by solution-enhanced dispersion by supercritical CO2[J]. *J Supercrit Fluids*, 2012, 67: 7-13.

[7] Sheth P, Sandhu H, Singhal D, lynnetwwwdagriorglynnet. Nanoparticles in the Pharmaceutical Industry and the Use of Supercritical Fluid Technologies for Nanoparticle Production[J]. *Curr Drug Deliv*, 2012, 9(3): 269-284.

[8] Bhavyasri K, Rambabu D, Prasad P S S, lynnetwwwdagriorglynnet. Separation of the two enantiomers of Gatifloxacin by SFC on amylose based stationary phase[J]. *J Chem Pharm Res*, 2012, 4(11): 4915-4920.

[9] Haimer E, Wendland M, Potthast A, lynnetwwwdagriorglynnet. Precipitation of Hemicelluloses from DMSO/Water Mixtures Using Carbon Dioxide as an Antisolvent[J]. *Journal of nanomaterials*, 2008.

[10] Zhang Y, Zhao X H, Li W G, lynnetwwwdagriorglynnet. Preparation, Characterization, and Dissolution Rate In Vitro Evaluation of Total Panax Notoginsenoside Nanoparticles, Typical Multicomponent Extracts from Traditional Chinese Medicine, Using Supercritical Antisolvent Process[J]. *Journal of nanomaterials*, 2015.

[11] Franceschi E, De Cesaro A M, Feiten M, lynnetwwwdagriorglynnet. Precipitation of β-carotene and PHBV and co-precipitation from SEDS technique using supercritical CO2[J]. *J Supercrit Fluids*, 2008, 47(2): 259-269.

[12] Miguel F, Martin A, Gamse T, lynnetwwwdagriorglynnet. Supercritical anti solvent precipitation of lycopene - Effect of the operating parameters[J]. *Journal of Supercritical Fluids*, 2006, 36(3): 225-235.

[13] Chang S-C, Lee M-J, Lin H-M. Role of phase behavior in micronization of lysozyme via a supercritical anti-solvent process[J]. *Chemical Engineering Journal*, 2008, 139(2): 416-425.

[14] Xiao K F, Wang W Q, Hu D D, lynnetwwwdagriorglynnet. Preparation of Cefquinome Nanoparticles by Using the Supercritical Antisolvent Process[J]. *Journal of nanomaterials*, 2015.

[15] Pan Y, Wang X, Liu X. Modern Dry Technology[M]. Beijing: Chemical Industry Press, 2007: 280-299.